

Constraints on Running of Non-Gaussianity from Large Scale Structure Probes

Ji-Ping Dai,¹ Jun-Qing Xia,^{1*}

¹*Department of Astronomy, Beijing Normal University, Beijing, 100875, China*

Accepted 2019 November 4. Received 2019 October 28; in original form 2019 September 16

ABSTRACT

In this letter we present constraints on the scale-dependent “local” type primordial non-Gaussianity, which is described by non-Gaussianity’s spectral index n_{NG} , from the NRAO VLA Sky Survey and the quasar catalog of the Sloan Digital Sky Survey (SDSS) Data Release 6, together with the SDSS Data Release 12 photo-z sample. Here, we use the auto-correlation analyses of these three probes and their cross-correlation analyses with the cosmic microwave background (CMB) temperature map, and obtain the tight constraint on the spectral index: $n_{\text{NG}} = 0.2^{+0.7}_{-1.0}$ (1σ C.L.), which shows the first competitive constraint on the running of non-Gaussianity from current large-scale structure clustering data. Furthermore, we also perform the forecast calculations and improve the limit of n_{NG} using the future Euclid mission, and obtain the standard deviation at 68% confidence level: $\Delta n_{\text{NG}} = 1.74$ when considering the fiducial value $f_{\text{NL}} = 3$, which provides the complementary constraining power to those from the CMB bispectrum information.

Key words: cosmology: theory – inflation – large-scale structure of universe

1 INTRODUCTION

The standard inflationary paradigm predicts a flat Universe perturbed by nearly Gaussian and scale invariant primordial perturbations. These predictions have been confirmed by the increasingly precise measurements of the CMB and the large-scale structure (LSS). Since the last decade, the Planck satellite has confirmed that the initial seeds of structure must have been close to Gaussian (Ade et al. 2016). However, it is difficult to discriminate between the vast array of inflationary scenarios since most of the present constraints on the Lagrangian of the inflaton field have been obtained from measurements of the two-point function, or power spectrum. Therefore, it is natural to study the non-Gaussianity signatures in higher order correlators.

Considering the non-Gaussianity, the bispectrum of gravitational potential $\Phi(\mathbf{k})$ is defined as,

$$\langle \Phi(\mathbf{k}_1) \Phi(\mathbf{k}_2) \Phi(\mathbf{k}_3) \rangle \equiv (2\pi)^3 \delta_D(\mathbf{k}_{123}) B_\Phi(k_1, k_2, k_3), \quad (1)$$

where $\delta_D(\mathbf{k}_{123}) \equiv \delta_D(\mathbf{k}_1 + \mathbf{k}_2 + \mathbf{k}_3)$ is the Dirac delta function, and

$$B_\Phi(k_1, k_2, k_3) \equiv f_{\text{NL}} F(k_1, k_2, k_3), \quad (2)$$

where f_{NL} is the amplitude of bispectrum, and F encodes the functional dependence on the specific triangle configurations. Here, we mainly focus on the “local” shape

which comes from the “squeezed” triangles dominantly ($k_3 \ll k_1, k_2$).

As shown by Grossi et al. (2009) in numerical simulations with non-Gaussian initial conditions of the local kind, the large-scale halo bias can be greatly affected by relatively small values of f_{NL} , which provides another way to test the primordial non-Gaussianity using the properties of the LSS clustering data. Based on this point, many works used the auto-correlation power spectrums or auto-correlation functions of high-redshift probes to constrain f_{NL} because the primordial non-Gaussianity can significantly enhance the clustering power at large scales (Xia et al. 2010a,b, 2011; Nikoloudakis et al. 2013; Karagiannis et al. 2014; Leistedt et al. 2014; Alvarez et al. 2014). These works obtained comparable results with the limits from the CMB bispectrum.

Even though a scale independent f_{NL} has been widely studied in recent works, a scale-dependent f_{NL} is still well-motivated by theoretical predictions of some inflationary models (Chen 2005; Khoury & Piazza 2009; Byrnes et al. 2010a,b, 2011; Riotto & Sloth 2011). To denote the running of f_{NL} , a non-Gaussianity’s spectral index n_{NG} is defined in analogy to the power spectrum spectral index. The first detailed forecasts on the running of non-Gaussianity were obtained by Sefusatti et al. (2009), and then by other works (Becker et al. 2012; Biagetti et al. 2013; Giannantonio et al. 2012), in which they performed the forecast analysis using the Fisher matrix method. Becker & Huterer (2012) took the first step and constrained the non-Gaussianity’s spectral in-

* E-mail: xiajq@bnu.edu.cn

dex using the WMAP bispectrum with KSW bispectrum estimator, $n_{\text{NG}} = 0.3^{+0.8}_{-0.6}$ at 68% confidence level. [Oppizzi et al. \(2018\)](#) extended their work and included additional shapes and running models, and got $n_{\text{NG}} = 0.4^{+0.8}_{-0.7}$ (1 σ C.L.) for the “local” shape considered in this letter. Recently, Planck collaboration published their new constraints on n_{NG} using the same method ([Akrami et al. 2018](#)), the results give a large error ($\Delta n_{\text{NG}} \sim 2$ for a constant prior) on this parameter because f_{NL} constrained by Planck is close to 0.

The main purpose of this letter is to constrain the running of the “local” type non-Gaussianity using the clustering information of LSS probes. Following [Byrnes et al. \(2010b\)](#), we parameterize the initial bispectrum with the two scalar fields inflationary model, where both fields contribute to the generation of the perturbations.

$$B_{\Phi}(k_1, k_2, k_3) = 2f_{\text{NL}} \times \left[\left(\frac{\sqrt{k_1 k_2}}{k_p} \right)^{n_{\text{NG}}} P_{\Phi}(k_1) P_{\Phi}(k_2) + 2\text{Perm} \right], \quad (3)$$

where k_p is the pivot point, and P_{Φ} is the primordial gravitational potential power spectrum. This kind of template arises, for example, from the mixed inflaton-curvaton scenario.

In contrast to previous works ([Sefusatti et al. 2009](#); [Biagetti et al. 2013](#)), we use the real LSS clustering data including radio sources from the NRAO VLA Sky Survey (NVSS) ([Condon et al. 1998](#)) and the quasar catalogue of the Sloan Digital Sky Survey Release 6 (SDSS DR6 QSOs) ([Richards et al. 2008](#)), as well as the low redshift probe SDSS Data Release 12 photo- z sample (SDSS DR12 PZs) ([Beck et al. 2016](#)). We constrain on the running of the “local” type non-Gaussianity using the auto-correlation power spectra (ACPS) C_{ℓ}^{qq} of these three LSS surveys, and their cross-correlation power spectra (CCPS) C_{ℓ}^{qT} with the CMB temperature fluctuations from the Planck observation.

2 FORMALISM

We assume that the collapsed objects form in extreme peaks of the density field $\delta(\mathbf{x}) = \delta\rho/\rho$. The statistics of collapsed objects can be described by the statistics of the density perturbation smoothed on some mass scale M . Following [LoVerde et al. \(2008\)](#), the non-Gaussianity probability density function can be obtained by the Edgeworth expansion ([Bernardeau et al. 2002](#)), where the non-Gaussianity mass function is

$$\mathcal{N}^{\text{NG}} = \frac{dn(M, z)}{dM} = -\sqrt{\frac{2}{\pi}} \frac{\bar{\rho}}{M} e^{-\frac{\delta_c^2}{2\sigma_M^2}} \left[\frac{d \ln \sigma_M}{dM} \times \left(\frac{\delta_c}{\sigma_M} + \frac{S_3 \sigma_M}{6} \left(\frac{\delta_c^4}{\sigma_M^4} - 2 \frac{\delta_c^2}{\sigma_M^2} - 1 \right) \right) + \frac{1}{6} \frac{dS_3}{dM} \sigma_M \left(\frac{\delta_c^2}{\sigma_M^2} - 1 \right) \right], \quad (4)$$

The redshift dependence is carried by the threshold for collapse $\delta_c(z) \approx 1.686/D(z)$, with $D(z)$ the growth factor. It worth noticing that we may replace δ_c with $\delta_{ec} = \sqrt{q}\delta_c$ for ellipsoidal collapse, and the correction $q = 0.75$ results from the N-body simulation ([Grossi et al. 2009](#)). σ_M^2 is the variance of the smoothed density fluctuation, and S_3 is the skewness which defines as $S_3 = \langle \delta_M^3 \rangle_c / \langle \delta_M^2 \rangle_c^2$. Taking Eq.(3) into the

above equation, we can calculate the correction on the Gaussianity mass function when considering the running non-Gaussianity model.

For the “local” type primordial non-Gaussianity, there are several theoretical expressions for the large-scale bias ([Afshordi & Tolley 2008](#); [Dalal et al. 2008](#); [Matarrese & Verde 2008](#); [Slosar et al. 2008](#); [McDonald 2008](#); [Desjacques et al. 2011a,b](#); [Scoccimarro et al. 2012](#)). In our analysis, we use the accurate prediction for the scale dependent bias correction from primordial non-Gaussianity ([Desjacques et al. 2011a](#)).

$$\Delta b(M, z, k) = 2 \frac{\mathcal{F}(M, k)}{W_M(k)M(k)} \left(b_L^G \delta_c(z) + \frac{1}{D(z)} \frac{d \ln \mathcal{F}(M, k)}{d \ln \sigma_M} \right) \quad (5)$$

where W_M is a top-hat windows function in Fourier space, and $M(k) = 2k^2 T(k) / (3\Omega_m H_0^2)$, in which $T(k)$ is the transfer function, Ω_m is the current fraction of the matter energy density, and H_0 is the current Hubble constant. b_L^G is the Gaussian Lagrangian bias and the shape function $\mathcal{F}(M, k)$ can be written as

$$\mathcal{F}(M, k) = \frac{1}{4\sigma_M^2 P_{\Phi}(k)} \int \frac{d^3 q}{(2\pi)^3} W_M(q) M(q) W_M(|\mathbf{k} - \mathbf{q}|) \times M(|\mathbf{k} - \mathbf{q}|) B_{\Phi}(k, q, |\mathbf{k} - \mathbf{q}|), \quad (6)$$

which includes the dependence of f_{NL} and n_{NG} . When setting $n_{\text{NG}} = 0$, $\mathcal{F}(M, k)$ returns to the constant f_{NL} at large scales as expected. It worth noticing that Eq.(6) is applied to the two scalar fields inflationary model, instead of the single scalar field model discussed in [Becker & Huterer \(2012\)](#), because in the single scalar field model there is a very strong degeneracy between f_{NL} and n_{NG} . Consequently, we can not obtain reasonable constraints on the latter from current LSS observations.

Making the standard assumption that halos move coherently with the underlying dark matter, the Lagrangian bias is related to the Eulerian one as $b = 1 + b_L$. We assume the large scale, linear halo bias for the Gaussian case is ([Sheth & Tormen 1999](#))

$$1 + b_L^G = 1 + \frac{1}{D(z_0)} \left[\frac{q \delta_c(z_f)}{\sigma_M^2} - \frac{1}{\delta_c(z_f)} \right] + \frac{2p}{\delta_c(z_f) D(z_0)} \left\{ 1 + \left[\frac{q \delta_c^2(z_f)}{\sigma_M^2} \right]^p \right\}^{-1} \quad (7)$$

where z_f is the halo formation redshift, and z_0 is the halo observation redshift. As we are interested in massive halos, we expect that $z_f \simeq z_0$. Here, $q = 0.75$ and $p = 0.3$ account for non-spherical collapse and are a fit result from numerical simulations ([Scoccimarro et al. 2001](#)).

Finally, in order to get the effective bias, we need to integrate the halo mass in the given range relevant to our sources,

$$b_{\text{eff}}^{\text{NG}}(M_{\text{min}}, z, k) = \frac{\int_{M_{\text{min}}}^{\infty} b^{\text{NG}}(M, z, k) \mathcal{N}^{\text{NG}}(M, z) dM}{\int_{M_{\text{min}}}^{\infty} \mathcal{N}^{\text{NG}}(M, z) dM}, \quad (8)$$

where $b^{\text{NG}}(M, z, k) = 1 + b_L^G(M, z) + \Delta b(M, z, k)$ is the scale-dependent bias. This effective bias is dependent on the minimal halo mass which differs for different sources.

2.1 Data Analysis

Since the Limber approximation is accurate below the

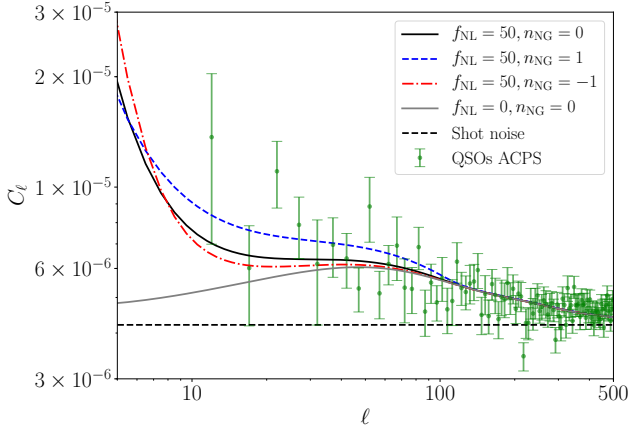


Figure 1. Observed ACPS of QSO sample, together with theoretical power spectra using different values of the non-Gaussianity and its running. The black dashed line denotes the shot-noise level in this QSO catalog.

level of 10% at $\ell > 10$ where we mainly focus on. It is sufficient for the present analysis. Here we use the public code CAMB¹ (Lewis et al. 2000) and implement the Limber approximation to calculate the ACPS and CCPS for LSS surveys (Limber 1953; Ho et al. 2008):

$$C_\ell^{gs} = \int dz \left[b_{\text{eff}}^{\text{NG}}(z) \frac{dN}{dz}(z) D(z) \right]^2 \frac{H(z)}{c\eta^2} P \left(k = \frac{\ell + 1/2}{\eta} \right), \quad (9)$$

$$C_\ell^{gT} = \frac{3\Omega_m H_0^2 T_{\text{CMB}}}{c^3 (\ell + 1/2)^2} \int dz b_{\text{eff}}^{\text{NG}}(z) \frac{dN}{dz}(z) D(z) H(z) \times \frac{d}{dz} \left(\frac{D(z)}{a(z)} \right) P \left(k = \frac{\ell + 1/2}{\eta} \right), \quad (10)$$

where dN/dz is the normalized selection function of the survey, η is the conformal lookback time, and T_{CMB} is the average temperature of CMB photons.

In our work, we use the high redshift probes, NVSS and SDSS DR6 QSOs, together with the low redshift probe SDSS DR12 PZs. Their redshift ranges span $0 < z < 3.5$, $0 < z < 5$, $0 < z < 1$, respectively, and we divide them into 200 bins uniformly to calculate the ACPS and CCPS. We refer to the recent work (Cuoco et al. 2017) for more details of these samples, including redshift distributions and masks. It is worth mentioning that several new quasar catalogs have been published based on the SDSS data release, complemented in some cases with additional information. Cuoco et al. (2017) has checked the adequacy of these different QSO samples, and showed that all these new samples were detected large variations in the number density of sources across the sky. Therefore, here we still rely on the SDSS DR6 QSOs catalog. The catalog of extragalactic objects are 2D pixelized maps of $n(\hat{\Omega}_i)$, with $N_{\text{side}} = 512$. We can use PolSpice² (Szapudi et al. 2001; Chon et al. 2004; Efstathiou 2004; Challinor & Chon 2005) to estimate the power spectra. Considering the ACPS, the shot-noise should be taken into

account; it is constant in multipole and can be expressed as $C_N = 4\pi f_{\text{sky}}/N_{\text{gal}}$, where f_{sky} is the fraction of sky covered by the catalog in the unmasked area and N_{gal} is the number of catalog objects in the unmasked area.

In order to show the effects of non-Gaussianity and its running, in Fig. 1 we present both the theoretical and observed (green points) ACPS, together with shot noise of DR6 QSOs sample (black dashed line). As we can easily see, when comparing the Gaussian case (grey solid line), a positive non-Gaussianity (black solid line) can significantly enhance the clustering power at large scales ($\ell < 60$). When including the non-zero non-Gaussianity's spectral index n_{NG} , the behaviors of ACPS at large scales become different. A positive n_{NG} obviously raises the amplitude of ACPS at scales $10 < \ell < 60$ as shown in the blue dashed line, while it plays the opposite way when n_{NG} is negative (red dash-dotted line). This discrepancy is the reason why we could use the LSS clustering data to constrain the non-Gaussianity and its non-Gaussianity's spectral index.

3 FITTING RESULTS

In our calculations, we use the public software CosmoMC³ (Lewis & Bridle 2002), a Markov Chain Monte Carlo (MCMC) code to perform the global constraints on f_{NL} and n_{NG} from the ACPS and CCPS clustering data at scales $10 < \ell < 500$ of three LSS surveys described above. Here, we abandon the very large scale data mainly for three reasons: 1) to avoid the deviation from accurate theory when we use Limber approximation. 2) to reduce the systematic error at very large scales. 3) to avoid the effects of gauge corrections on the power spectrum on very large scales (Yoo et al. 2009). A simple χ^2 is used for the fit in our analysis:

$$\chi^2 = \sum_{i \text{th data}} \sum_{\ell} (\hat{C}_\ell^i - C_\ell^i)^T \Gamma_i^{-1} (\hat{C}_\ell^i - C_\ell^i), \quad (11)$$

where Γ_i are the covariance matrixes output from PolSpice estimator and i means different ACPS or CCPS when we perform the the joint analysis. \hat{C}_ℓ^i and C_ℓ^i represent the model and the measured power spectrum. Furthermore, we also constrain three minimal halo masses M_{min} for three LSS surveys, and the constraint results on M_{min} using their ACPS and CCPS are $10^{12.5 \pm 0.09} h^{-1} M_\odot$ for NVSS, $10^{12.1 \pm 0.1} h^{-1} M_\odot$ for SDSS DR6 QSOs and $10^{11.5 \pm 0.21} h^{-1} M_\odot$ for SDSS DR12 PZs, respectively (1σ C.L.). In order to accelerate the calculation, we do not include the basic cosmological parameters. We admit there are degeneracies between some of the cosmological parameters with f_{NL} , but they are constrained very tight by Planck. We have checked our work, and the results show these parameters have very little influence on the final constraints. Therefore, we assume the standard Λ CDM model, with purely adiabatic initial conditions and a flat Universe, and fix the six cosmological parameters as best fit values from the Planck measurement (Aghanim et al. 2018): $\Omega_b h^2 = 0.0224$, $\Omega_c h^2 = 0.1201$, $100\theta_{\text{MC}} = 1.0409$, $\tau = 0.0543$, $n_s = 0.9661$, $\ln(10^{10} A_s) = 3.0448$.

Oppizzi et al. (2018) showed the dependence of the likelihood on the pivot scale k_p . As Becker & Huterer (2012)

¹ <http://camb.info>

² <http://www2.iap.fr/users/hivon/software/PolSpice/>

³ <http://cosmologist.info/cosmomc/>

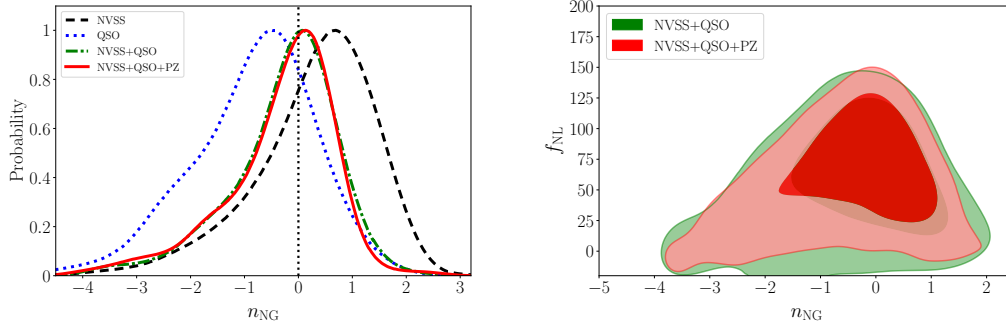


Figure 2. Marginalized one-dimensional distributions of n_{NG} and two-dimensional distributions ($1, 2\sigma$ contours) of n_{NG} and f_{NL} using different datasets. See text for more details.

Table 1. Constraints on n_{NG} and f_{NL} from different datasets, together with constraints from WMAP bispectrum.

	f_{NL}			n_{NG}		
	best fit	1σ	2σ	best fit	1σ	2σ
NVSS ACPS	51	[10, 106]	[-53, 144]	0.8	[-0.9, 1.8]	[-2.9, 2.5]
NVSS ACPS+CCPS	53	[14, 103]	[-31, 144]	0.9	[-0.7, 1.8]	[-2.8, 2.4]
QSO ACPS	43	[-7, 108]	[-84, 135]	-0.7	[-2.1, 0.7]	[-3.8, 1.4]
QSO ACPS+CCPS	41	[-4, 107]	[-82, 134]	-0.6	[-1.9, 0.6]	[-3.6, 1.4]
NVSS+QSO ACPS+CCPS	54	[28, 101]	[-18, 132]	0.1	[-0.9, 0.9]	[-2.5, 1.6]
NVSS+QSO+PZ ACPS+CCPS	58	[31, 103]	[-13, 133]	0.2	[-0.8, 0.9]	[-2.4, 1.4]
WMAP7 (Becker & Huterer 2012)	—	—	—	0.3	[-0.3, 1.1]	[-0.9, 2.2]
WMAP9 (Oppizzi et al. 2018)	—	—	—	0.4	[-0.3, 1.2]	—

proposed, the true pivot scale favored by the data is the value of k_p for which the errors in f_{NL} and n_{NG} are uncorrelated. In our analysis, we start with an arbitrary value of k_p , compute the likelihood and then rescale k_p by (Shandera et al. 2011),

$$k_p = k_p^* \exp\left(-\frac{C_{f_{\text{NL}}, n_{\text{NG}}}^*}{f_{\text{NL}}^* C_{n_{\text{NG}}, n_{\text{NG}}}^*}\right), \quad (12)$$

where k_p^* is the arbitrary pivot used initially and f_{NL}^* is the constraint result using k_p^* , C is the covariance matrix between f_{NL}^* and n_{NG}^* . In practice, we find $k_p = 0.016 \text{Mpc}^{-1}$ is appropriate in our analysis, since the degeneracy between f_{NL} and n_{NG} we obtain is small enough if using this pivot scale.

We start with the NVSS catalog. In Tab. 1 we list constraints on n_{NG} and f_{NL} from NVSS. If only using the NVSS ACPS, we obtain the constraint: $f_{\text{NL}} = 51_{-41}^{+55}$ (1σ C.L.), which is consistent with the Gaussian case at 2σ confidence level, similar with previous works. The non-Gaussianity's spectral index can also be constrained by the ACPS data: $n_{\text{NG}} = 0.8_{-1.7}^{+1.0}$ at 68% C.L., which is consistent with zero at 1σ confidence level, and implies that a positive value is slightly preferred, since in the analysis we find that there is a mild enhancement on the amplitudes of ACPS data points at scales $\ell < 30$. When we combine the ACPS and CCPS of NVSS together, the constraint on n_{NG} is slightly tightened: $n_{\text{NG}} = 0.9_{-1.6}^{+0.9}$ at 1σ confidence level, as shown in the black

dashed line in Fig. 2. Apparently, in this analysis the constraining power of ACPS is much stronger than the CCPS.

Then we move to the SDSS DR6 QSOs data. Similar with the NVSS result, using ACPS data alone the constraint of non-Gaussianity is consistent with zero safely: $f_{\text{NL}} = 43_{-50}^{+65}$ (1σ C.L.). This result is different from some previous works (Xia et al. 2011), which might due to the more conservative mask we use in the analysis. We also obtain the constraint on the non-Gaussianity's spectral index: $n_{\text{NG}} = -0.7_{-1.4}^{+1.4}$ (1σ C.L.), which is also consistent with zero at 1σ confidence level. Unlike the NVSS constraint, the DR6 QSO sample slightly prefers a negative value of n_{NG} , since the ACPS data points at scales $10 < \ell < 100$ are slightly suppressed comparing with the non-running case. Again, we combine the ACPS and CCPS of SDSS DR6 QSOs, the blue dotted line shows that the constraint only has a very minor change: $n_{\text{NG}} = -0.6_{-1.3}^{+1.2}$ at 68% confidence level. The non-running case is still favored by the QSO data.

If we combine the ACPS and CCPS data of NVSS and SDSS DR6 QSOs samples together, we obtain tight constraint on the non-Gaussianity's spectral index: $n_{\text{NG}} = 0.1_{-1.0}^{+0.8}$ ($1, \sigma$ C.L.), as shown in the green dash-dotted line, which shows a constraint competitive to previous work (Becker & Huterer 2012; Oppizzi et al. 2018) that used the CMB bispectrum to constrain the running non-Gaussianity. In the right panel of Fig. 2, we also show the two-dimensional contours between f_{NL} and n_{NG} . Clearly we can see that now the degeneracy between them is not very strong, since we

set a proper scale k_p in the calculations. Furthermore, we also see a long tail at lower values of n_{NG} , because in our calculations we only use the data points at $\ell > 10$. The effect of the negative n_{NG} is smaller than that of the positive non-Gaussianity's spectral index at scales $10 < \ell < 100$, as shown in Fig. 1. Therefore, the constraining power on the negative n_{NG} will be weaker than that on the positive index. Finally, we add the ACPS and CCPS of SDSS DR12 PZs into the analysis, and obtain a tight constraint on the non-Gaussianity's spectral index of the "local" type non-Gaussianity:

$$n_{\text{NG}} = 0.2_{-1.0}^{+0.7} \quad (1\sigma \text{ C.L.}), \quad (13)$$

which clearly shows that the non-running case is supported by the current LSS clustering data.

Here we also preform a simple forecast using the future Euclid observation to estimate constraints on f_{NL} and n_{NG} based on the Fisher matrix technique. The Fisher matrix for the running non-Gaussianity parameters f_{NL} and n_{NG} is given by (Biagetti et al. 2013)

$$\mathcal{F}_{ij} = V_{\text{surv}} f_{\text{sky}} \int \frac{dk k^2}{2\pi^2} \frac{1}{2P_g^2} \frac{\partial P_g}{\partial \theta_i} \frac{\partial P_g}{\partial \theta_j}, \quad (14)$$

where θ_i are f_{NL} and n_{NG} in our analysis, V_{surv} is the surveyed volume, and f_{sky} is the fraction of the sky observed. The integral over the momenta runs from $k_{\text{min}} = 2\pi/(V_{\text{surv}} f_{\text{sky}})^{1/3}$ to $k_{\text{max}} = 0.03h\text{Mpc}^{-1}$, above which the non-Gaussian bias becomes negligible. Including shot-noise, the galaxy power spectrum $P_g(k)$ can be

$$P_g(k, z) = b_{\text{eff}}^2(k, z) P_m(k, z) + \frac{1}{\bar{n}} \quad (15)$$

where \bar{n} is the mean number density of the survey. In our analysis, we assume the fiducial values $f_{\text{NL}} = 3$ and $n_{\text{NG}} = 0$ ruled by Planck (Akrami et al. 2018). We also use the minimal halo mass $M_{\text{min}} = 10^{13} M_{\odot}$ and the pivot scale $k_p = 0.016\text{Mpc}^{-1}$. We have adopted the specification from Euclid (Laureijs et al. 2011), $z_{\text{median}} = 0.9$, $f_{\text{sky}} = 0.48$, $V_{\text{surv}} = 190h^{-3}\text{Gpc}^3$, together with the number density of 30 galaxies per square arcminute. Finally, we obtain the standard deviations of the non-Gaussianity and its non-Gaussianity's spectral index are $\Delta n_{\text{NG}} = 1.74$ and $\Delta f_{\text{NL}} = 4.2$. In the future, the LSS clustering data can also provide the complementarity constraining power on the non-Gaussianity's spectral index.

4 CONCLUSIONS

In this letter, we analyze the effects of the running of "local" type non-Gaussianity, originated from the general two scalar fields model, on mass function, large scale halo bias and correlation angular power spectrum comprehensively. The non-Gaussianity's spectral index n_{NG} has effect on the LSS clustering data at large scale. Therefore, we use the current LSS data: NVSS and SDSS DR6 QSOs as high redshift probes, together with SDSS DR12 PZs as lower redshift probe to compute their ACPS and CCPS with CMB map. Combining all data together, we obtain the first tight constraint on the non-Gaussianity's spectral index from the current LSS data: $n_{\text{NG}} = 0.2_{-1.0}^{+0.7}$ (1σ C.L.) at the pivot scale $k_p = 0.016\text{Mpc}^{-1}$. We also perform a forecast for n_{NG} using

the future Euclid survey, which shows that the LSS clustering data can also useful on the estimation of the non-Gaussianity spectral's index of "local" type non-Gaussianity.

ACKNOWLEDGEMENTS

J.-Q. Xia is supported by the National Science Foundation of China under grants No. U1931202, 11633001, and 11690023; the National Key R&D Program of China No. 2017YFA0402600; the National Youth Thousand Talents Program and the Fundamental Research Funds for the Central Universities, grant No. 2017EYT01.

REFERENCES

- Ade P., et al., 2016, *Astronomy & Astrophysics*, 594, A17
 Afshordi N., Tolley A. J., 2008, *Physical Review D Particles & Fields*, 78, 220
 Aghanim N., et al., 2018, arXiv preprint arXiv:1807.06209
 Akrami Y., et al., 2018, arXiv preprint arXiv:1807.06211
 Alvarez M., et al., 2014, arXiv preprint arXiv:1412.4671
 Beck R., Dobos L., Budavári T., Szalay A. S., Csabai I., 2016, *Monthly Notices of the Royal Astronomical Society*, 460, 1371
 Becker A., Huterer D., 2012, *Physical review letters*, 109, 121302
 Becker A., Huterer D., Kadota K., 2012, *Journal of Cosmology and Astroparticle Physics*, 2012, 034
 Bernardeau F., Colombi S., Gaztanaga E., Scoccimarro R., 2002, *Physics reports*, 367, 1
 Biagetti M., Perrier H., Riotto A., Desjacques V., 2013, *Physical Review D*, 87, 063521
 Byrnes C. T., Nurmi S., Tasinato G., Wands D., 2010a, *Journal of Cosmology and Astroparticle Physics*, 2010, 034
 Byrnes C. T., Gerstenlauer M., Nurmi S., Tasinato G., Wands D., 2010b, *Journal of Cosmology and Astroparticle Physics*, 2010, 004
 Byrnes C. T., Enqvist K., Nurmi S., Takahashi T., 2011, *Journal of Cosmology and Astroparticle Physics*, 2011, 011
 Challinor A., Chon G., 2005, *Monthly Notices of the Royal Astronomical Society*, 360, 509
 Chen X., 2005, *Physical Review D*, 72, 123518
 Chon G., Challinor A., Prunet S., Hivon E., Szapudi I., 2004, *Monthly Notices of the Royal Astronomical Society*, 350, 914
 Condon J. J., Cotton W., Greisen E., Yin Q., Perley R., Taylor G., Broderick J., 1998, *The Astronomical Journal*, 115, 1693
 Cuoco A., Bilicki M., Xia J.-Q., Branchini E., 2017,] 10.3847/1538-4365/aa8553
 Dalal N., Doré O., Huterer D., Shirokov A., 2008, *Phys. Rev. D*, 77, 123514
 Desjacques V., Jeong D., Schmidt F., 2011a, *Physical Review D*, 84, 061301
 Desjacques V., Jeong D., Schmidt F., 2011b, *Physical Review D*, 84, 063512
 Efstathiou G., 2004, *Monthly Notices of the Royal Astronomical Society*, 348, 885
 Giannantonio T., Porciani C., Carron J., Amara A., Pillepich A., 2012, *Monthly Notices of the Royal Astronomical Society*, 422, 2854
 Grossi M., Verde L., Carbone C., Dolag K., Branchini E., Iannuzzi F., Matarrese S., Moscardini L., 2009, *Monthly Notices of the Royal Astronomical Society*, 398, 321
 Ho S., Hirata C., Padmanabhan N., Seljak U., Bahcall N., 2008, *Phys. Rev. D*, 78, 043519
 Karagiannis D., Shanks T., Ross N. P., 2014, *MNRAS*, 441, 486
 Khoury J., Piazza F., 2009, *Journal of Cosmology and Astroparticle Physics*, 2009, 026

- Laureijs R., et al., 2011, arXiv preprint arXiv:1110.3193
- Leistedt B., Peiris H. V., Roth N., 2014, *Physical Review Letters*, **113**, 221301
- Lewis A., Bridle S., 2002, *Physical Review D*, **66**, 103511
- Lewis A., Challinor A., Lasenby A., 2000, *apj*, **538**, 473
- Limber D. N., 1953, *The Astrophysical Journal*, **117**, 134
- LoVerde M., Miller A., Shandera S., Verde L., 2008, *Journal of Cosmology and Astroparticle Physics*, 2008, 014
- Matarrese S., Verde L., 2008, *The Astrophysical Journal*, **677**, L77
- McDonald P., 2008, *Physical Review D*, **78**, 123519
- Nikoloudakis N., Shanks T., Sawangwit U., 2013, *MNRAS*, **429**, 2032
- Oppizzi F., Liguori M., Renzi A., Arroja F., Bartolo N., 2018, *Journal of Cosmology and Astroparticle Physics*, 2018, 045
- Richards G. T., et al., 2008, *The Astrophysical Journal Supplement Series*, **180**, 67
- Riotto A., Slotth M. S., 2011, *Physical Review D*, **83**, 041301
- Scoccimarro R., Sheth R. K., Hui L., Jain B., 2001, *The Astrophysical Journal*, **546**, 20
- Scoccimarro R., Hui L., Manera M., Chan K. C., 2012, *Physical Review D*, **85**, 083002
- Sefusatti E., Liguori M., Yadav A. P., Jackson M. G., Pajer E., 2009, *Journal of Cosmology and Astroparticle Physics*, 2009, 022
- Shandera S., Dalal N., Huterer D., 2011, *Journal of Cosmology and Astroparticle Physics*, 2011, 017
- Sheth R. K., Tormen G., 1999, *Monthly Notices of the Royal Astronomical Society*, **308**, 119
- Slosar A., Hirata C., Seljak U., Ho S., Padmanabhan N., 2008, *Journal of Cosmology and Astroparticle Physics*, 2008, 031
- Szapudi I., Prunet S., Colombi S., 2001, *The Astrophysical Journal Letters*, **561**, L11
- Xia J.-Q., Viel M., Baccigalupi C., De Zotti G., Matarrese S., Verde L., 2010a, *The Astrophysical Journal Letters*, **717**, L17
- Xia J.-Q., Bonaldi A., Baccigalupi C., De Zotti G., Matarrese S., Verde L., Viel M., 2010b, *Journal of Cosmology and Astroparticle Physics*, 2010, 013
- Xia J.-Q., Baccigalupi C., Matarrese S., Verde L., Viel M., 2011, *Journal of Cosmology and Astroparticle Physics*, 2011, 033
- Yoo, J., Fitzpatrick, A. L., & Zaldarriaga, M. 2009, *Physical Review D*, **80**, 083514

This paper has been typeset from a $\text{\TeX}/\text{\LaTeX}$ file prepared by the author.